

NJC

Accepted Manuscript



This is an *Accepted Manuscript*, which has been through the Royal Society of Chemistry peer review process and has been accepted for publication.

Accepted Manuscripts are published online shortly after acceptance, before technical editing, formatting and proof reading. Using this free service, authors can make their results available to the community, in citable form, before we publish the edited article. We will replace this *Accepted Manuscript* with the edited and formatted *Advance Article* as soon as it is available.

You can find more information about *Accepted Manuscripts* in the [Information for Authors](#).

Please note that technical editing may introduce minor changes to the text and/or graphics, which may alter content. The journal's standard [Terms & Conditions](#) and the [Ethical guidelines](#) still apply. In no event shall the Royal Society of Chemistry be held responsible for any errors or omissions in this *Accepted Manuscript* or any consequences arising from the use of any information it contains.

Cite this: DOI: 10.1039/c0xx00000x

www.rsc.org/xxxxxx

PAPER

Towards efficient blue emission cationic Ir(III) complex with azole-type ancillary ligands: a joint theoretical and experimental study

Shao-Fen Huang, Hai-Zhu Sun, Guo-Gang Shan*, Yong Wu, Min Zhang* and Zhong-Min Su*

Received (in XXX, XXX) Xth XXXXXXXXX 200X, Accepted Xth XXXXXXXXX 200X

DOI: 10.1039/b000000x

Pyridine-azole moieties have been proved to be an attractive building block for multifunctional cationic Ir(III) complexes, however, few highly efficient blue materials are demonstrated and the deep structure-properties relationships need to be revealed. Herein, a series of cationic $[\text{Ir}(\text{dfppz})_2(\text{N}^{\wedge}\text{N})][\text{PF}_6]$ complexes (**1–4**) based on azole-type ancillary ligand, namely, 1,1'-diphenyl-1*H*,1'*H*-[2,2'] biimidazolyl (Phbid), 2-(1-phenyl-1*H*-imidazol-2-yl)-pyridine (Bpyim), 2-(1-methyl-1*H*-imidazol-2-yl)-pyridine (Mpyim), and 2-(1,5-dimethyl-1*H*-[1,2,4]triazole-3-yl)-pyridine (Mpytz), respectively, have been prepared and their photophysical, electrochemical and charge transporting properties are investigated. The reported complexes exhibit strong perceived green to blue emission as well as excellent redox reversibility at room temperature. The comprehensive density functional theory calculations are performed to provide insight into the electronic structures of **1–4** and disclose the ancillary ligand effect on the emission behavior in detail. The simple methyl group modification endow the triazole-type ancillary with exceedingly large π - π^* energy gap, resulting blue emitting complex **4**, namely $[\text{Ir}(\text{dfppz})_2(\text{Mpytz})][\text{PF}_6]$ with peak value at 462 nm. Meanwhile, despite the significant ^3LC character, the high efficiency with quantum yield of 31.6% of **4** is realized in neat film, which is higher than those of reported cationic Ir(III) complexes with similar emissions. Additionally, the calculation results also suggest that complexes **2–4** possess better electron-transporting abilities in comparison with that of **1**.

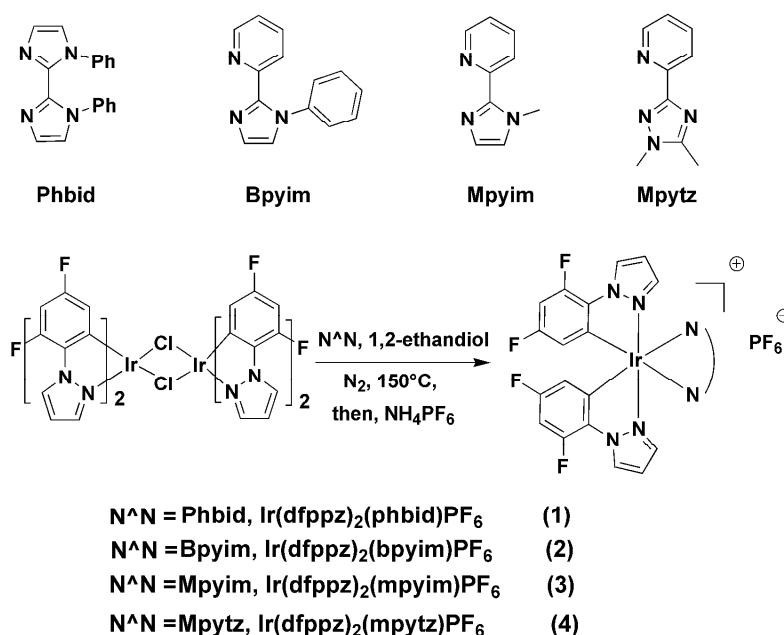
Introduction

Phosphorescent transition-metal complexes have attracted enormous interest during the past decade because of their potential applications in academic research and practical application.^{1–3} Such phosphors can harvest both singlet and triplet excitons due to heavy atom induced spin-orbit coupling effect, thus leading to high phosphorescence quantum efficiency.^{4–8} Among all kinds of phosphorescent complexes, cyclometalated Ir(III) complexes have emerged as the most promising candidates as a result of their synthetic versatility, good photo- and thermal stabilities, relatively short excited-state lifetime, convenient emission wavelength tunability as well as high efficiency.^{9–13} Up to now, the reported Ir(III) complexes can be generally classified into two categories, namely neutral Ir(III) complexes and cationic Ir(III) complexes. Recently, many efforts have been devoted to investigating the latter ones with the formula of $\text{Ir}(\text{II})(\text{C}^{\wedge}\text{N})_2(\text{N}^{\wedge}\text{N})^+$, which are balanced by the counter anions such as PF_6^- , BF_4^- , Cl^- , on account of their wide applications in chemical and biological sensors, photo-driven water splitting and optoelectronic devices in particular.^{14–20} Thanks to the intrinsically ionic character of cationic Ir(III) complexes, they have been successfully used as emitting layer in solid-state light-emitting electrochemical cells (LECs) with advantages of solution-process, single-layer and air-stable cathodes.^{21–26}

Benefiting from appealing characteristics of LECs, extensive researches have been conducted on the design and synthesis of

cationic Ir(III) complexes through ingenious ligand control to achieve high efficiency and modify the emission color ultimately.^{27, 28} Increasing steric hindrance of ligands has been proved to be an effective way to improve quantum efficiency.^{29, 30} As for emission color, the green, yellow, orange and red emitting cationic Ir(III) complexes have been exploited widely.^{31–34} In contrast, the number of blue emitting cationic Ir(III) complexes is rather limited, despite the efficient blue ones are essential components for full-color displaying and solid-state lighting.^{11, 35} Moreover, it is noted that the synthesized cationic Ir(III) complexes should have excellent charge-transporting ability and high phosphorescence quantum efficiency to realize stable and efficient lighting. Otherwise, the LECs will not work or exhibit low efficiency, which is relation with the structural feature of LECs as revealed in the previous reports.³⁶ Thereby, the exploitation of more efficient cationic blue Ir(III) complexes, and investigation of the relationships between the structure and properties are highly desired.

Previous works indicate that the imidazole-type moieties as ancillary ligands can facilitate the construction of the efficient cationic Ir(III) complexes with higher emission energies.^{37–40} In addition, such units are easily synthesized and modified via grafting the functional groups. Imidazole-type moieties are thus used as a promising building block to synthesize Ir(III) complexes with tunable photophysical and charge-transfer properties. Recently, we developed a series of multifunctional



Scheme 1. Chemical structures of studied ancillary ligands and synthetic routes of complexes 1–4.

cationic Ir(III) complexes based on 1,2,4-triazole-pyridine type ancillary ligands.^{41–43} These complexes exhibit high phosphorescence quantum efficiencies in the neat films, however, the emission colors are not in region of blue-emitting, even 1-(2,4-difluoro-phenyl)-1H-pyrazole (dfppz) showing the large π - π^* energy gap is used as cyclometalated ligand. The possible reason is that the introduced moieties on 1,2,4-triazole-pyridine ancillary ligands such as phenyl ring possess extended conjugation, giving smaller energy gap and red-shifted emission of the resulting complexes. It is supposed that if the conjugation can be reduced, the blue-emitting cationic Ir(III) dyes will be constructed. Herein a simple methyl unit was chosen to modify 1,2,4-triazole-pyridine ancillary ligands as its weak conjugation and electron-donating ability. Keeping this in mind, a new ancillary ligand, 2-(1,5-dimethyl-1H-[1,2,4]triazole-3-yl)-pyridine (Mpytz) was synthesized, as shown in scheme 1. Using dfppz as cyclometalated ligand, complex $[\text{Ir}(\text{dfppz})_2(\text{Mpytz})][\text{PF}_6]$ (4) is readily prepared. In addition, we also employ other imidazole-based ancillary ligands, 1,1'-diphenyl-1H,1'H-[2,2']biimidazolyl (Phbid), 2-(1-phenyl-1H-imidazol-2-yl)-pyridine (Bpyim) and 2-(1-methyl-1H-imidazol-2-yl)-pyridine (Mpyim), to explore their changes of emission color, excited-state properties and the charge-transporting abilities.

In this paper, the synthesis, characterization, photophysical and electrochemical properties of studied cationic Ir(III) complexes 1–4, have been described in detail. All complexes show strong phosphorescence at room temperature with the emission wavelength in range from 517 to 460 nm. The photophysical behaviors are interpreted with the help of the comprehensive density functional theory calculations. The obtained results further demonstrate that they show comparable charge-transporting properties. Importantly, it shows that complex 4 with Mpytz ligands are blue-emitting material in its neat film with PLQY of 31.6 %, higher than reported cationic Ir(III) complexes with similar emissions in the films.

Experimental

General procedure

Commercial reagents were used as received unless specially stated. The solvents for syntheses were freshly distilled over appropriate drying reagents. All experiments were performed under a nitrogen atmosphere using standard Schlenk techniques. ¹H NMR spectra were recorded on Bruker Avance 500 MHz spectrometer with tetramethylsilane as internal standard. UV-Vis absorption spectra were recorded on a Cary 500 spectrometer. Photoluminescence spectra of all complexes were obtained through the F-4600 FL spectrophotometer. The PLQYs of the neat film were measured in an integrating sphere. The thermogravimetric analyses (TGA) were performed on a Perkin-Elmer TG-7 analyzer heated from R.T. to 800 °C in flowing nitrogen.

Synthesis

The ligands used in this work were expediently synthesized according to the reported literatures procedure.^{37, 41} The corresponding ¹H NMR data for all ligands are presented in the electronic supplementary information (ESI).† All complexes were obtained by analogy reactions of reported precedent.³⁷

Synthesis of complexes

Hdfppz (0.90 g, 5.00 mmol) and $\text{IrCl}_3 \cdot 3\text{H}_2\text{O}$ (0.70 g, 2.00 mmol) were dissolved in a mixture of 2-ethoxyethanol/water (16 mL, 3:1 V/V) solution. The reaction mixture was degassed repeatedly and refluxed for 20 h while protected from light and oxygen. The reaction was cooled down to room temperature and 5 mL of water was added. The resulted solid was filtered and washed with 25 mL water, 25 mL ethanol and 25 mL diethyl ether (Et_2O), then dried *in vacuo*. The crude dichloro-bridged diiridium complex was used without any further purification. A suspension of μ -dichloro bridged iridium-dimer (0.15 g, 0.10 mmol) and desired

ancillary ligand (0.27 mmol) in 16 mL ethane-1,2-diol was degassed by multiple vacuum and N₂ purging cycles and stirred at 150 °C for 20 h, protected from light. The reaction mixture was cooled down to room temperature and diluted with water subsequently. An aqueous solution of NH₄PF₆ was added to afford the desired precipitate. The resulted solid was filtered and further purified *via* silica gel column chromatography and recrystallized from dichloromethane and petroleum ether.

[(dfppz)₂Ir(phbid)] PF₆ (1)

A white solid in 65% yield. ¹H NMR (d₆-DMSO, 500 MHz) δ (ppm): 8.62 (s, 2H), 8.39 (d, *J* = 8.0 Hz, 1H), 8.23 (t, *J* = 8.0 Hz, 1H), 8.03 (d, *J* = 5.5 Hz, 1H), 7.70 (s, 1H), 7.59 (t, *J* = 2.5 Hz, 1H), 7.27 (d, *J* = 2.5 Hz, 1H), 7.24 (d, *J* = 2.5 Hz, 1H), 7.13–7.05 (m, 2H), 6.79–6.77 (m, 2H), 6.69 (s, 1H), 5.71–5.70 (m, 1H), 4.25 (s, 3H). MS (MALDI-TOF): *m/z* 837.2 (M–PF₆).

[(dfppz)₂Ir(bpyim)] PF₆ (2)

A slight yellow solid in 52% yield. ¹H NMR (d₆-DMSO, 500 MHz) δ (ppm): 8.66 (t, *J* = 3.3 Hz, 2H), 8.03 (t, *J* = 8.8 Hz, 1H), 7.98 (t, *J* = 4.5 Hz, 1H), 7.92 (d, *J* = 1.5 Hz, 1H), 7.75 (s, 5H), 7.53–7.50 (m, 2H), 7.40 (d, *J* = 2.5 Hz, 1H), 7.11–7.10 (m, 2H), 6.93–6.90 (m, 2H), 6.84–6.82 (m, 2H), 5.69–5.66 (m, 2H). MS (MALDI-TOF): *m/z* 802.2 (M–PF₆).

[(dfppz)₂Ir(mpyim)] PF₆ (3)

A slight yellow solid in 55% yield. ¹H NMR (d₆-DMSO, 500 MHz) δ (ppm): 8.62 (s, 2H), 8.39 (d, *J* = 8.0 Hz, 1H), 8.23 (t, *J* = 8.0 Hz, 1H), 8.03 (d, *J* = 5.5 Hz, 1H), 7.70 (s, 1H), 7.59 (t, *J* = 2.5 Hz, 1H), 7.27 (d, *J* = 2.5 Hz, 1H), 7.24 (d, *J* = 2.5 Hz, 1H), 7.13–7.05 (m, 2H), 6.79–6.77 (m, 2H), 6.69 (s, 1H), 5.71–5.70 (m, 1H), 4.25 (s, 3H). MS (MALDI-TOF): *m/z* 740.2 (M–PF₆).

[(dfppz)₂Ir(mpytz)] PF₆ (4)

A white solid in 38% yield. ¹H NMR (d₆-DMSO, 500 MHz) δ (ppm): 8.67 (t, *J* = 3.3 Hz, 2H), 8.37 (d, *J* = 8.0 Hz, 1H), 8.28 (t, *J* = 7.8 Hz, 1H), 7.92–7.88 (m, 2H), 7.67 (t, *J* = 6.8 Hz, 1H), 7.34 (d, *J* = 2.5 Hz, 1H), 7.20–7.10 (m, 2H), 6.88 (t, *J* = 2.5 Hz, 1H), 6.80 (t, *J* = 2.8 Hz, 1H), 5.64–5.62 (m, 1H), 5.54 (t, *J* = 3.8 Hz, 1H), 3.25 (s, 3H), 2.52 (s, 3H). MS (MALDI-TOF): *m/z* 725.1 (M–PF₆).

X-ray crystallography

Single crystals suitable for X-ray diffraction analyses were successfully gained except for complex 3 through slow vapor diffusion from the corresponding complexes solution in a mixture of CH₂Cl₂/Et₂O/CH₃OH (5:3:2, in volume). The single-crystal X-ray diffraction data for complexes 1, 2 and 4 were collected on a Bruker Apex CCD II area-detector diffractometer with graphite structures were all solved by Direct Method of SHELXS-97 and refined by full-matrix least-square techniques using the

SHELXL-97 program in WINGX.⁴² The hydrogen atoms of aromatic rings were included in the structure factor calculation at idealized positions by using a riding model. Anisotropic thermal parameters were used to refine all non-hydrogen atoms except for part of nitrogen and carbon atoms. The solvent molecules are highly disordered, and attempts to locate and refine the solvent peaks were unsuccessful. Contributions to scattering due to these solvent molecules were removed by using the SQUEEZE routine of PLATON; structures were then refined again using the data generated.

Theoretical calculations

The geometrical structures of the ground and the lowest triplet states (T₁) for all complexes were fully optimized with C1 symmetry constraints by using the restricted closed-shell and open-shell B3LYP methods, respectively. The “Double-ξ” quality basis sets were employed for C, H, N atoms (6-31G*) and Ir atom (LANL2DZ). The effective core potential (ECP) replaced the inner core electrons of iridium leaving the outer core (5s)²(5p)⁶ electrons and the (5d)⁶ valence electrons of iridium(III). The expectation values calculated for S² were smaller than 2.05 in the spin-unrestricted calculation. To improve the influence of triplet instabilities in time-dependent DFT (TD-DFT), Tamm-Dancoff Approximation (TDA) in TD-DFT calculations was performed in the presence of the solvent (CH₃CN) at the optimized T₁ geometry.^{45,46} All calculations reported here were carried out with the Gaussian 09 software package.⁴⁷

Electrochemistry

Cyclic voltammetry (CV) was performed on a BAS 100 W instrument with a scan rate of 100 mV s⁻¹ in acetonitrile using tetrabutylammonium hexafluorophosphate (0.1 M) as the supporting electrolyte and ferrocene as the internal standard. The analytic system adopted the three-electrode configuration with a glassy carbon electrode as the working electrode, an aqueous saturated calomel electrode as the operating reference electrode and a platinum wire as the counter electrode.

Results and discussions

Synthesis of the studied complexes

The studied complexes were synthesized in moderate yields of 38% to 65%. The products were prepared through traditional two steps method. The column chromatograph method were applied to purified the crude products. The products were characterized by ¹H-NMR and the structures of 1, 2 and 4 were confirmed by single crystal structures.

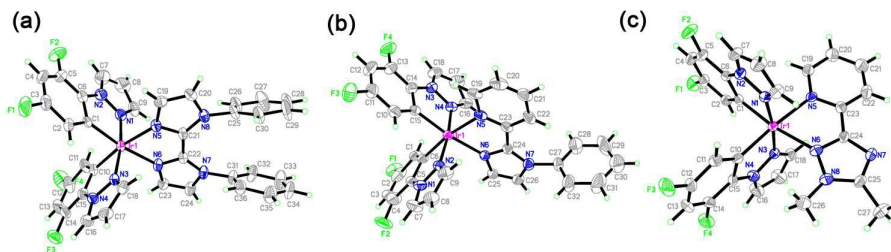


Fig. 1. ORTEP diagram of complexes 1, 2 and 4 with thermal ellipsoids shown at the 30% probability level. The relevant solvent molecules, counter anions (PF₆⁻) are omitted for clarity.

X-ray single crystal structure

The single crystal structures of complexes **1**, **2** and **4** are illustrated in Fig. 1 and the detailed data are listed in Table S1–S2†. It is obvious that these complexes show almost octahedral geometry with minor distortion coordinating with two cyclometalated ligands (dfppz) and one auxiliary ligand. All complexes examined show small bite angles, causing a slightly distorted octahedral geometry. Taking complex **1** as an example, two dfppz ligands exhibit a *trans*-arrangement of the N-donors and *cis*-arrangement of the C atoms which is unexceptionally consistent with the reported ionic Ir(III) complex.^{11, 29} The Ir–N bond lengths of cyclometalated ligands lie between 2.025(7) and 2.017(8) which are slightly longer than Ir–C distances 2.013(9) and 2.007(9). Owing to the strong Ir–C interaction of dfppz ligands, the ancillary ligand presents remarkable lengthened Ir–N distances of 2.137(7) and 2.140(7) compared to those trans-orientated Ir–N bonds of dfppz. We can find the similar phenomena for other two complexes in Table S2†.

Photophysical properties

The absorption and emission spectra of **1–4** in CH₃CN solution at room temperature were recorded and shown in Fig. 2. The numerical results are summarized in Table 1. As depicted in Fig. 2 (a), the intensive absorption ranging from 250 to 290 nm of them are mainly assigned to spin-allowed ¹π–π* transition of ligands. While the following weak absorption bands that occur at lower energy region extending from 290 to 400 nm can be ascribed to an association of ¹MLCT (metal to ligand charge-transfer), ³MLCT, ¹LLCT (ligand-to-ligand charge transfer), ³LLCT, and ligand-centered ³π–π* (³LC) transitions.^{48, 49} According to the spectral profiles, the absorption spectra can be categorized into three classes. Complexes **2** and **3** with same 1*H*-imidazolylpyridine fragment but various substitutes show similar absorption patterns with different intensity. The absorption spectra of **1** and **4** exhibit different profiles compared with those of **2** and **3**. The results indicate that the N[^]N fragments play a more important role on electron transition processes, while the substitutions on ancillary ligands have small effect on that.

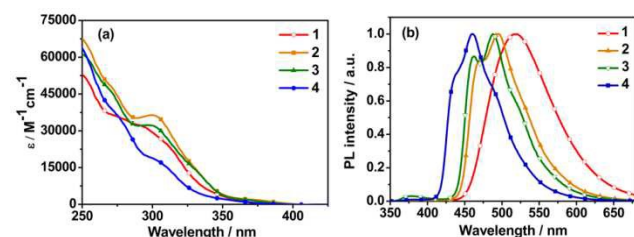


Fig. 2. (a) Absorption spectra and (b) photoluminescent spectra of complexes **1–4** in acetonitrile (10^{-5} M) at 298 K.

Table 1. Photophysical and electrochemical characteristics for **1–4**.

	$\lambda_{PL,max}$ (nm) ^{a, b}	Φ^b (%)	τ^b (μ s)	E_{ox}^c (V)	E_{red}^c (V)
1	517, 511	45.2	5.7	1.12	-2.28
2	495, 495	41.0	2.4	1.09	-2.21
3	487, 489	30.8	2.1	1.05	-2.26
4	460, 462	31.6	0.4	1.18	-2.26

^a Measured in CH₃CN (10^{-5} M) at 298 K. ^b Measured in the neat film. ^c Measured by CV with ferrocene as the standard.

To better understand the nature of the excited states involved in

their absorption spectra, the theoretical calculations based on optimized geometries have been undertaken. The corresponding calculated excited energies, dominant orbital excitations, and oscillator strength, configurations and relevant orbital distributions of **1** have been shown in Fig. 3 and data listed in Table 2. The data for **2–4** are shown in the ESI.† Taking complex **1** as an example, the simulated absorption spectrum of complex **1** is depicted in Fig. 3 (a), which is consistent well with the experimental spectrum profile. The occupied molecular orbitals participating in main excitations, HOMO (H), HOMO-1, HOMO-3 and HOMO-4 are predominantly localized on the cyclometalated ligand and iridium center, while HOMO-2 locates on ancillary ligand and iridium center. As for the lowest unoccupied orbital (LUMO), it resides on ancillary ligand together with contribution from iridium center in part. Energy region from 250 to 300 nm including bands 1 and 2 ascribe primarily to the excitation from H-5→L+1, H-3→L+1 and H-5→L, respectively. Consequently, the high energy absorption bands are mainly assigned to the π–π* transitions involving both cyclometalated and ancillary ligands. The calculated absorption bands 3 and 4 spreading from 310 to 400 nm are predominantly originated from H→L+1, H-4→L, H-2→L, characterized by MLCT, LLCT as well as additional IL states feature. These related attribution results agree with the experimental ones perfectly. Moreover, the similar assignments for the rest complexes can be obtained from our TD-DFT results as shown in Tables S3–S5†.

Table 2. Calculated excited energies of the excited state (ES), dominant orbital excitations, and oscillator strength (*f*) of complex **1** in CH₃CN solution from TD-DFT calculation.

	1	ES	eV/nm	<i>f</i>	Major contributions	Character
Band 1	S2	5	4.85/253	0.26	H-5→L+1 (37%)	LLCT/MLCT
					H-3→L+1 (12%)	IL
Band 2	S8	4.27/290	0.24	0.24	H-1→L+2 (11%)	IL
					H-5→L (79%)	IL/ LCT
Band 3	S4	3.98/312	0.05	0.05	H-2→L (14%)	IL/MLCT
					H→L+1 (88%)	IL/MLCT
					H-4→L (43%)	LLCT/MLCT
Ban 4	S	3.86/322	0.03	0.03	H-1→L (52%)	LLCT
					H-2→L (75%)	IL/MLCT
S1	3.41/364	0.01	0.01	0.01	H-5→L (16%)	IL/LLCT/MLCT
					H→L (96%)	MLCT/LLCT

⁷⁵ H and L denote HOMO and LUMO, respectively.

Fig. 2 (b) presents the photoluminescence spectra of **1–4** detected in acetonitrile at 298 K. Through ancillary ligands modification, complexes **1–4** possess progressively blue-shifted emissions with peak values at 517, 495, 487 and 460 nm, respectively, and are characterized by somewhat structured profiles with high energy shoulder except for **1**. Generally, the observed emissions for cationic Ir(III) complexes are assigned to ³MLCT, ³LLCT and LC ³π–π* excited-states or the mixed ones, which can be described as follows: $\Phi T = a\Phi(^3MLCT) + b\Phi(^3LLCT) + c\Phi(^3LC)$. Thereby, the emission spectra of cationic Ir(III) complexes commonly depend on the normalized coefficients of a, b and c. The broad and featureless emission is observed for the complexes with ³MLCT and ³LLCT characters, whereas ³LC character usually results in the vibronically structured emission spectra. Thus, we tentatively attribute the origin of the emission of **1** to ³MLCT and ³LLCT characters, and

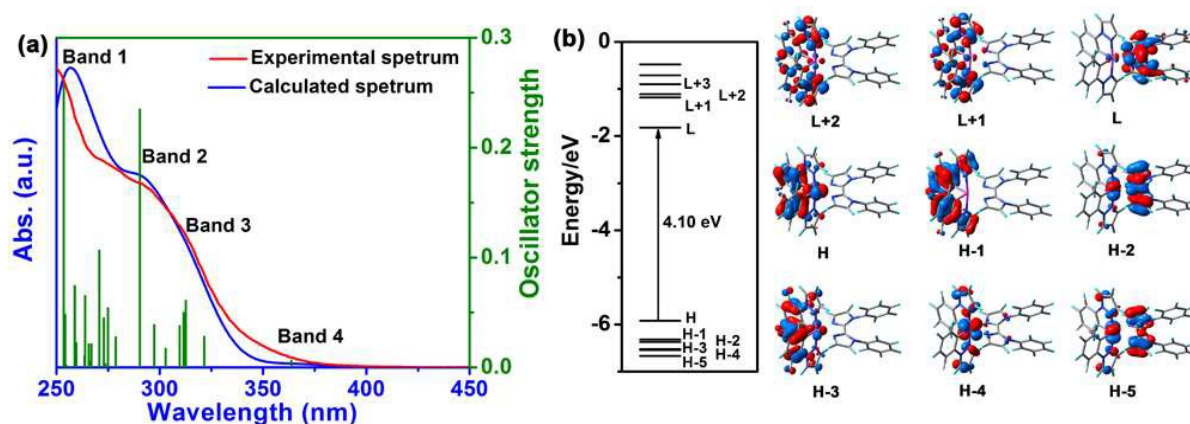


Fig. 3. (a) TD-DFT simulated and experimental absorption spectra of complex **1** in CH_3CN . (b) The shape of frontier electronic levels and selected frontier molecular orbitals involved in crucial electronic excitations of complex **1**. H and L denote HOMO and LUMO, respectively.

that the excited-states of **2–4** could have, in addition to $^3\text{MLCT}$ and $^3\text{LLCT}$, different degrees of ^3LC characters. Upon cooling the solutions down to 77 K, complex **2–4** show much more rigidochromic blue-shifts with respect to their emission at room temperatures. As for complex **1**, the broad and structureless photoluminescent spectrum is replaced by vibronically structured one accompanied by a considerable degree of blue-shift, which further demonstrates its excited states characters of $^3\text{MLCT}$ and $^3\text{LLCT}$. Combining the emission spectra at 298 K with those at 77 K (see Fig. S1), the results suggest that the emissions of **2–4** show a relatively large ^3LC component than that of **1**. Further evidences are supported by TD-DFT calculations approach and the obtained results are presented in Table S6†. Based on the theoretical data and photophysical characterizations, it is believed that their emissions should originate from $^3\text{MLCT}$ and $^3\text{LLCT}$ and ^3LC characters with different contributed proportion. The differences in electron density between T_1 and the ground state S_0 for **1–4** exhibited here further confirm the transition characters mentioned above (see Fig. 4).

To deep understand the effect of ancillary ligands on their emission behaviors, the formation of the frontier molecular orbitals of **1–4** by combining the valence orbitals of cyclometalated ligand and iridium atom, $[\text{Ir}(\text{CN})_2]^+$ and those of ancillary ligands, have been studied. As shown in Fig. S5, it is clear that the ancillary ligands of **1–3** contributed to their frontier molecular orbitals involved in emissions. The emission wavelengths of **1–3** are thus related to the energy gaps of their ancillary ligands. According to previous reports, if the ancillary ligand participates in the emissive excited-state, the emission color can be controlled by modifying the energy gap of ancillary ligand. The much larger energy gap usually leads to blue-shifted emission. From the view of the structure point, the conjugated phenyl rings in **1** and **2** may decrease the energy gaps of ancillary ligands, and hence the low-energy emissions of them with respect to that of **3**. Our calculated data further support this point (see Fig. S5). However, for complex **4**, the lowest lying excited state is mainly dominated by the part of $[\text{Ir}(\text{CN})_2]^+$ due to exceedingly large $\pi-\pi^*$ gap of ancillary ligand. This may explain why **4** possesses much more ^3LC component than others. It is noted that the higher-energy unoccupied orbital of $[\text{Ir}(\text{CN})_2]^+$ (LUMO+1) contributes the emission of **4**, which is not observed for

complexes **1–3**. The net result of these finding will further lead to the blue-shifted emission. Based on these experimental and theoretical results, it can conclude that if the energy gap of $[\text{Ir}(\text{CN})_2]^+$ is slightly large or close to that of ancillary ligand, the ancillary ligand can participate in the excited-state efficiently. Thereby, the emission colors of such complexes can be adjusted by the ancillary ligands. Once the energy gap of ancillary ligand is much large than that of $[\text{Ir}(\text{CN})_2]^+$, the $[\text{Ir}(\text{CN})_2]^+$ -controlled emission will be observed with relatively large ^3LC excited-state character. As a result, tuning the emission color of cationic Ir(III) complexes with large $\pi-\pi^*$ gap can be achieved by employing the various cyclometalated ligands, which may simplify the material designs and the synthetic task.

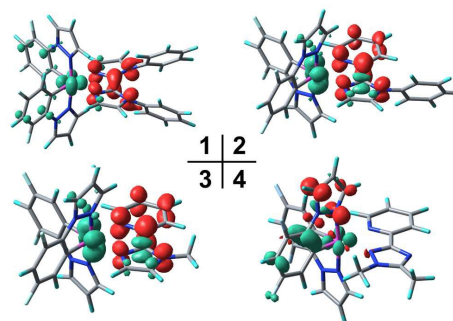


Fig. 4. Difference electron density computed by subtracting the electron densities of the T_1 and S_0 states for complexes **1–4**. The charge goes from the green to the red areas.

In the real-world application, the phosphorescent Ir(III) complexes are utilized as luminescent materials in their solid-state, for example, as thin films in the fabrication of the optoelectronic devices. However, the strong intermolecular interactions between the neighboring chromophores always result in larger red-shifted emission and decreased PLQY, which limits the development of the efficient blue-emitting materials. In addition, the efficiency of LECs can be evaluated from PLQY in the neat films of cationic Ir(III) complex in principle. To further investigate the photophysical properties in aggregation states, their emission spectra (see Fig. 5) and PLQYs in neat films were recorded, showing the considerable PLQYs. Encouragingly, complex **4** exhibits strong emission with PLQY of 30.6% and slightly red-shifted emission within 2 nm compared to the

photoluminescence in solution. Additionally, complex **1** exhibits the highest PLQY of 45.2% among all complexes, which might be attributed to the steric hindrance of phenyl groups on ancillary ligands and this hypothesis was supported by the decreasing PLQY along with the decreasing steric hindrance. All complexes exhibit microsecond timescale indicating their phosphorescent nature. Moreover, it is noteworthy that complex **4** possesses relative short lifetime (0.4 μ s), which may reduce the triplet-triplet annihilation in neat film and benefit it for the applications in LECs.⁵³

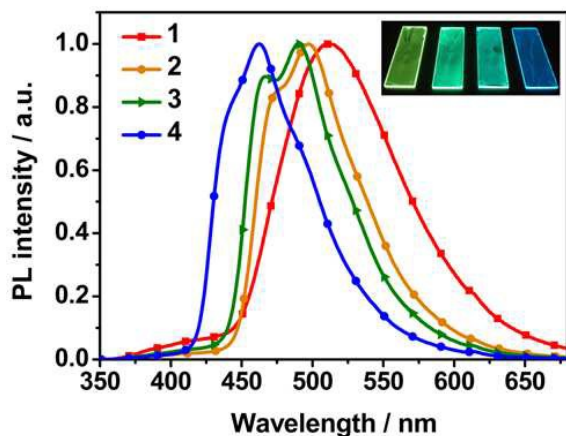


Fig. 5. Photoluminescent spectra of **1–4** in neat films.

Electrochemical properties

Electrochemical properties of complexes **1–4** were measured using cyclic voltammetry (Fig. S6†) and the redox potentials are presented in Table 1. All complexes exhibit reversible oxidation processes in CH₃CN, which is assigned to the oxidation of iridium metal cationic site [Ir(III)→Ir(IV)].⁵⁴ The complexes using in LECs require superior redox reversibility to transport both hole and electron. Although these complexes have identical cyclometalated ligand, their oxidation potentials reveal different values with 1.45, 1.40, 1.36 and 1.50 V, respectively, which demonstrates the effect of ancillary ligand on oxidation potential. According to the reported work, the HOMO mainly distributes on π_{C^N} and d orbitals of Ir center while the LUMO is on ancillary ligand.^{55, 56} The reduction processes are reversible for all complexes except for **1**. The reduction irreversibility of complex **1** might be attributed to ancillary ligand **Phbid** and the similar phenomena were observed in previous literature.³⁷ As the conjugation length decrease from complex **2** to **3**, the reduction potentials are shifted cathodically (by 170 mV), which indicates that the LUMO of complex **2** is tremendously stabilized by the phenyl moiety.

Thermal properties

The thermal stabilities of complexes **1–4** were evaluated by TGA under a stream of nitrogen with a scanning rate of 10 °C min⁻¹. The obtained results suggest that complexes **2–4** exhibit good thermal stabilities with high decomposition temperatures (T_d , corresponding to 5% weight loss) of 331, 344 and 357 °C, respectively, while complex **1** shows a relatively poor thermal properties with T_d of 230 °C. Generally, triazole-based ancillary ligand are proved to be better candidates to construct Ir(III)

complexes with high thermal stabilities than biimidazole ones.

Charge-transfer properties

It is well-known that the electron injection and transport properties of the materials play an important role on the device performance, especially single-layer devices such as LECs.⁵⁷ Both ionization potentials (IP) and electron affinities (EA) are the main factors in evaluating the efficiency of holes and electrons injection.^{58, 59} Herein, the theoretical calculation has been performed to explore the charge-transfer properties of complexes **1–4**. The calculated values of IP, EA together with hole extraction potential (HEP) and electron extraction potential (EEP) for them are listed in Table 3.

Table 3. Vertical ionization potential (IP), vertical electron affinity (EA), extraction potential (HEP and EEP) and intramolecular reorganization energy (λ_{hole} and $\lambda_{\text{electron}}$).

	IP (v)	HEP (v)	EA (v)	EEP (v)	λ_{hole}	$\lambda_{\text{electron}}$
1	9.24	9.13	3.06	3.83	0.11	0.77
2	9.40	9.30	3.41	3.97	0.10	0.56
3	9.50	9.40	3.52	3.93	0.10	0.41
4	9.72	9.53	3.38	3.86	0.19	0.48

The lower IP and higher EA are beneficial to injection of holes and electrons, respectively. As observed from Table 3, complex **1** exhibit smaller IP and EA value than others, indicating that **1** may have good holes-injection ability rather than electron-injection ability. **3** exhibits improved electron-injection ability in comparison with those of complex **1**, **2** and **4**, due to its higher EA value. Additionally, the charge transport rate strongly depends on the reorganization energy (λ) according to the Marcus electron transfer regime.^{60, 61} As reported in the previous works, the reorganization energy is determined by the inner reorganization energy (λ_i) and the external reorganization energy (λ_e). Usually, λ_i is dominant in λ because that the value of λ_e is very small. To study the charge-transfer rates of complexes **1–4**, their λ_i for the hole and electron were evaluated on basis of the following expressions, respectively.

$$\lambda_{\text{hole}} = \lambda^+ + \lambda^0 = [E^+(M^0) - E^+(M^+)] + [E^0(M^+) - E^0(M^0)] = \text{IP}(v) - \text{HEP}$$

$$\lambda_{\text{electron}} = \lambda^- + \lambda^0 = [E^-(M^0) - E^-(M^-)] + [E^0(M^-) - E^0(M^0)] = \text{EEP} - \text{EA}(v)$$

Clearly, they show almost identical hole reorganization energies (λ_{hole}), suggesting that the variation of ancillary ligand has little different on their λ_{hole} but it significantly changes the electron and hole injection abilities. The electron reorganization energies ($\lambda_{\text{electron}}$) of complexes **2–4** are obviously lower than that of complex **1**. This result suggests that **2–4** possess better electron-transporting abilities with respect to **1**.

Conclusion

A series of [Ir(dfppz)₂(N[^]N)]PF₆ complexes chelated with dfppz and different ancillary ligands have been successfully prepared and fully characterized by spectroscopic and electrochemical methods. The single crystal structures of complexes **1**, **2** and **4** have been elucidated. The use of different ancillary ligands successfully tunes the emission of studied complexes from green to blue. DFT calculations have been performed to rationalize the experimental spectroscopy and deeply understand their intrinsic charge-transfer properties. Different from complexes **1–3** with imidazole-type ligands, the

simple methyl group attached into complex **4** endow the triazole-pyridine type ligand with exceedingly large π - π^* energy gap, resulting in the $[\text{Ir}(\text{CN})_2]^+$ -controlled emission characterized by a relatively large ^3LC feature. Despite the presence of significant ^3LC character, the high efficiency in neat film of **4** is realized, which is higher than those of reported cationic Ir(III) complexes with similar emissions. We hope that the results obtained here can provide guidance for simplification of material design and the synthetic task, hence further develop more efficient blue emitting phosphors used in optical devices.

Acknowledgments

The authors gratefully acknowledge the financial support from NSFC (21303012, 21273030, 51203017 and 21131001), the Science and Technology Development Planning of Jilin Province (20130204025GX and 20130522167JH).

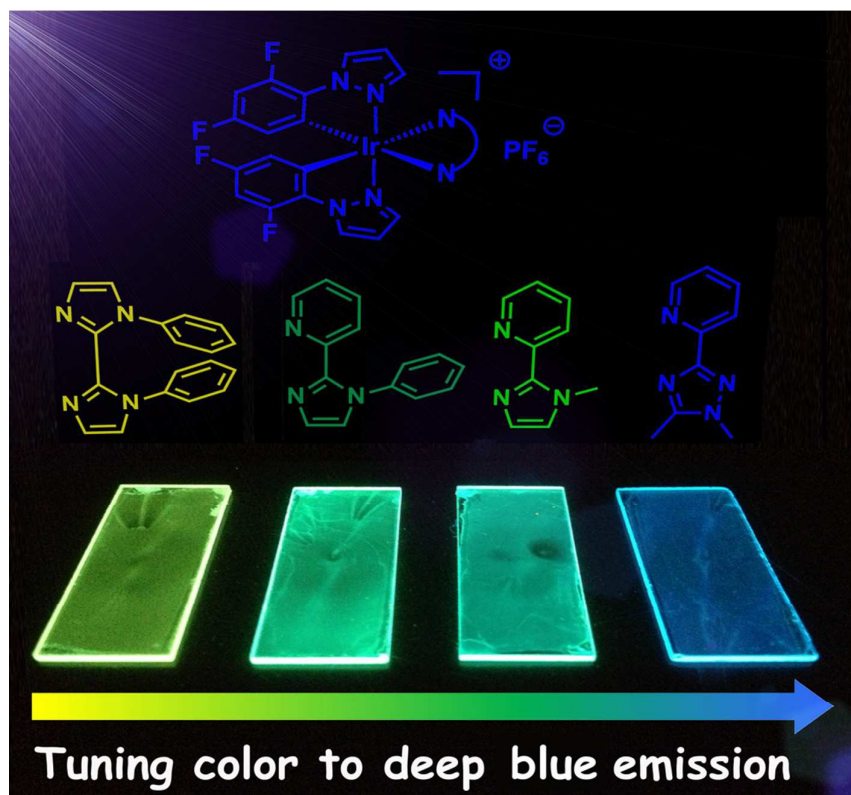
Notes and references

Institute of Functional Material Chemistry, faculty of chemistry, Northeast Normal University, Changchun, 130024 Jilin, People's Republic of China. E-mail: shangg187@nenu.edu.cn; mzhang@nenu.edu.cn, zmsu@nenu.edu.cn

†Electronic Supplementary Information (ESI) available: [Synthesis and characterization of the ligands used in this work, X-ray single crystal data, computational results and CV curves of complexes **1-4**]. See DOI: 10.1039/c000000x/

- R. D. Costa, E. Orti, H. J. Bolink, F. Monti, G. Accorsi and N. Armaroli, *Angew. Chem., Int. Ed.*, 2012, **51**, 8178.
- Y. Chi and P. T. Chou, *Chem. Soc. Rev.*, 2010, **39**, 638.
- Q. Zhao, F. Y. Li and C. H. Huang, *Chem. Soc. Rev.*, 2010, **39**, 3007.
- C. Adachi, M. A. Baldo, M. E. Thompson and S. R. Forrest, *J. Appl. Phys.*, 2001, **90**, 5048.
- S. Tokito, T. Iijima, T. Tsuzuki and F. Sato, *Appl. Phys. Lett.*, 2003, **83**, 2459.
- S. C. Lo, E. B. Namdas, P. L. Burn and I. D. W. Samuel, *Macromolecules*, 2003, **36**, 9721.
- H. J. Bolink, E. Coronado, R. D. Costa, N. Lardies and E. Orti, *Inorg. Chem.*, 2008, **47**, 9149.
- Q. Wang, J. Q. Ding, D. G. Ma, Y. X. Cheng, L. X. Wang, X. B. Jing and F. S. Wang, *Adv. Funct. Mater.*, 2009, **19**, 84.
- C. H. Chang, Z. J. Wu, C. H. Chiu, Y. H. Liang, Y. S. Tsai, J. L. Liao, Y. Chi, H. Y. Hsieh, T. Y. Kuo, G. H. Lee, H. A. Pan, P. T. Chou, J. S. Lin and M. R. Tseng, *ACS Appl. Mater. & Inter.*, 2013, **5**, 7341.
- C. F. Chang, Y. M. Cheng, Y. Chi, Y. C. Chiu, C. C. Lin, G. H. Lee, P. T. Chou, C. C. Chen, C. H. Chang and C. C. Wu, *Angew. Chem., Int. Ed.*, 2008, **47**, 4542.
- L. He, L. Duan, J. Qiao, R. J. Wang, P. Wei, L. D. Wang and Y. Qiu, *Adv. Funct. Mater.*, 2008, **18**, 2123.
- E. Baranoff, H. J. Bolink, E. C. Constable, M. Delgado, D. Haussinger, C. E. Housecroft, M. K. Nazeeruddin, M. Neuberger, E. Orti, G. E. Schneider, D. Tordera, R. M. Walliser and J. A. Zampese, *Dalton Trans.*, 2013, **42**, 1073.
- V. V. Grushin, N. Herron, D. D. LeCloux, W. J. Marshall, V. A. Petrov and Y. Wang, *Chem. Commun.*, 2001, 1494.
- D. R. Whang, K. Sakai and S. Y. Park, *Angew. Chem., Int. Ed.*, 2013, **52**, 11612.
- X. G. Hou, Y. Wu, H. T. Cao, H. Z. Sun, H.-B. Li, G. G. Shan and Z.-M. Su, *Chem. Commun.*, 2014, **50**, 6031.
- A. Tsuboyama, H. Iwakaki, M. Furugori, T. Mukaide, J. Kamatani, S. Igawa, T. Moriyama, S. Miura, T. Takiguchi, S. Okada, M. Hoshino and K. Ueno, *J. Am. Chem. Soc.*, 2003, **125**, 12971.
- H. Zeng, F. Yu, J. Dai, H. Sun, Z. Lu, M. Li, Q. Jiang and Y. Huang, *Dalton Trans.*, 2012, **41**, 4878.
- X. Li, T. N. Zang, H. J. Chi, Y. Dong, G. Y. Xiao and D. Y. Zhang, *Dyes Pigments*, 2014, **106**, 51.
- Y. H. Song, Y. C. Chiu, Y. Chi, Y. M. Cheng, C. H. Lai, P. T. Chou, K. T. Wong, M. H. Tsai and C. C. Wu, *Chemistry*, 2008, **14**, 5423.
- W. Y. Wong, G. J. Zhou, X. M. Yu, H. S. Kwok and B. Z. Tang, *Adv. Funct. Mater.*, 2006, **16**, 838.
- J. Keruckas, J. V. Grazulevicius, D. Volyniuk, V. Cherpak and P. Stakhira, *Dyes Pigments*, 2014, **100**, 66.
- J. M. F. Hernandez, S. Ladouceur, Y. L. Shen, A. Iordache, X. R. Wang, L. Donato, S. Gallagher-Duval, M. D. Villa, J. D. Slinker, L. De Cola and E. Zysman-Colman, *J. Mater. Chem. C*, 2013, **1**, 7440.
- G. E. Schneider, A. Pertegas, E. C. Constable, C. E. Housecroft, N. Hostettler, C. D. Morris, J. A. Zampese, H. J. Bolink, J. M. Junquera-Hernandez, E. Orti and M. Sessolo, *J. Mater. Chem. C*, 2014, **2**, 7047.
- D. Tordera, J. J. Serrano-Perez, A. Pertegas, E. Orti, H. J. Bolink, E. Baranoff, M. K. Nazeeruddin and J. Frey, *Chem. Mater.*, 2013, **25**, 3391.
- S. B. Meier, W. Sarfert, J. M. Junquera-Hernandez, M. Delgado, D. Tordera, E. Orti, H. J. Bolink, F. Kessler, R. Scopelliti, M. Gratzel, M. K. Nazeeruddin and E. Baranoff, *J. Mater. Chem. C*, 2013, **1**, 58.
- Y. Li, N. Dandu, R. Liu, Z. Li, S. Kilina and W. Sun, *J. Phys. Chem. C*, 2014, **118**, 6372.
- H. F. Chen, W. Y. Hung, S. W. Chen, T. C. Wang, S. W. Lin, S. H. Chou, C. T. Liao, H. C. Su, H. A. Pan, P. T. Chou, Y. H. Liu and K. T. Wong, *Inorg. Chem.*, 2012, **51**, 12114.
- K. Y. Lu, H. H. Chou, C. H. Hsieh, Y. H. Yang, H. R. Tsai, H. Y. Tsai, L. C. Hsu, C. Y. Chen, I. C. Chen and C. H. Cheng, *Adv. Mater.*, 2011, **23**, 4933.
- L. He, L. A. Duan, J. A. Qiao, G. F. Dong, L. D. Wang and Y. Qiu, *Chem. Mater.*, 2010, **22**, 3535.
- T. Hu, L. Duan, J. Qiao, L. He, D. Q. Zhang, L. D. Wang and Y. Qiu, *Synth. Met.*, 2013, **163**, 33.
- B. Liang, C. Y. Jiang, Z. Chen, X. J. Zhang, H. H. Shi and Y. Cao, *J. Mater. Chem.*, 2006, **16**, 1281.
- H. J. Tang, Y. H. Li, Q. L. Chen, B. Chen, Q. Q. Qiao, W. Yang, H. B. Wu and Y. Cao, *Dyes Pigments*, 2014, **100**, 79.
- D. Tordera, A. Pertegas, N. M. Shavaleev, R. Scopelliti, E. Orti, H. J. Bolink, E. Baranoff, M. Gratzel and M. K. Nazeeruddin, *J. Mater. Chem.*, 2012, **22**, 19264.
- J. Q. Ding, J. Gao, Y. X. Cheng, Z. Y. Xie, L. X. Wang, D. G. Ma, X. B. Jing and F. S. Wang, *Adv. Funct. Mater.*, 2006, **16**, 575.
- P. Coppo, M. Duati, V. N. Kozhevnikov, J. W. Hofstraat and L. De Cola, *Angew. Chem., Int. Ed.*, 2005, **44**, 1806.
- X. B. Xu, X. L. Yang, Y. Wu, G. J. Zhou, C. Wu and W. Y. Wong, *Chem.-Asian J.*, 2015, **10**, 252.
- L. He, J. Qiao, L. Duan, G. F. Dong, D. Q. Zhang, L. D. Wang and Y. Qiu, *Adv. Funct. Mater.*, 2009, **19**, 2950.
- E. Baranoff, S. Fantacci, F. De Angelis, X. X. Zhang, R. Scopelliti, M. Gratzel and M. K. Nazeeruddin, *Inorg. Chem.*, 2011, **50**, 451.
- C. D. Sunesh, G. Mathai and Y. Choe, *ACS Appl. Mater. Interfaces*, 2014, **6**, 17416.
- C. D. Sunesh, G. Mathai and Y. Choe, *Org. Electron*, 2014, **15**, 667.
- G. G. Shan, H. B. Li, H. T. Cao, H. Z. Sun, D. X. Zhu and Z. M. Su, *Dyes Pigments*, 2013, **99**, 1082.
- G. G. Shan, H. B. Li, H. T. Cao, D. X. Zhu, P. Li, Z. M. Su and Y. Liao, *Chem. Commun.*, 2012, **48**, 2000.
- G. G. Shan, H. B. Li, D. X. Zhu, Z. M. Su and Y. Liao, *J. Mater. Chem.*, 2012, **22**, 12736.
- L. J. Farrugia, *WINGX, A Windows Program for Crystal Structure Analysis*, University of Glasgow, Glasgow, UK, 1988.
- M. J. G. Peach, M. J. Williamson and D. J. Tozer, *J. Chem. Theory Comput.*, 2011, **7**, 3578.
- R. M. Edkins, K. Fucke, M. J. G. Peach, A. G. Crawford, T. B. Marder and A. Beeby, *Inorg. Chem.*, 2013, **52**, 9842.
- M. J. Frisch, G. W. Trucks, H. B. Schlegel, G. E. Scuseria, M. A. Robb, J. R. Cheeseman, G. Scalmani, V. Barone, B. Mennucci, G. A. Petersson, H. Nakatsuji, M. Caricato, X. Li, H. P. Hratchian, A. F. Izmaylov, J. Bloino, G. Zheng, J. L. Sonnenberg, M. Hada, M. Ehara, K. Toyota, R. Fukuda, J. Hasegawa, M. Ishida, T. Nakajima, Y. Honda, O. Kitao, H. Nakai, T. Vreven, J. A. Montgomery Jr, J. E.

- Peralta, F. Ogliaro, M. Bearpark, J. J. Heyd, E. Brothers, K. N. Kudin, V. N. Staroverov, R. Kobayashi, J. Normand, K. Raghavachari, A. Rendell, J. C. Burant, S. S. Iyengar, J. Tomasi, M. Cossi, N. Rega, J. M. Millam, M. Klene, J. E. Knox, J. B. Cross, V. Bakken, C. Adamo, J. Jaramillo, R. Gomperts, R. E. Stratmann, O. Yazyev, A. J. Austin, R. Cammi, C. Pomelli, J. W. Ochterski, R. L. Martin, K. Morokuma, V. G. Zakrzewski, G. A. Voth, P. Salvador, J. J. Dannenberg, S. Dapprich, A. D. Daniels, O. Farkas, J. B. Foresman, J. V. Ortiz, J. Cioslowski and D. J. Fox, *Gaussian 09, Revision A.02; Gaussian, Inc., Wallingford CT*, 2009.
48. H. J. Bolink, L. Cappelli, E. Coronado, A. Parham and P. Stossel, *Chem. Mater.*, 2006, **18**, 2778.
49. Q. Zhao, M. X. Yu, L. X. Shi, S. J. Liu, C. Y. Li, M. Shi, Z. G. Zhou, C. H. Huang and F. Y. Li, *Organometallics*, 2010, **29**, 1085.
- 15 50. J. Li, Peter I. Djurovich, Bert D. Alleyne, M. Yousufuddin, N. N. Ho, J. C. Thomas, Jonas C. Peters, Robert Bau and M. E. Thompson, *Inorg. Chem.*, 2005, **44**, 1713.
51. F. Monti, A. Baschieri, I. Gualandi, J. J. Serrano-Perez, J. M. Junquera-Hernandez, D. Tonelli, A. Mazzanti, S. Muzzioli, S. Stagni, C. Roldan-Carmona, A. Pertegas, H. J. Bolink, E. Orti, L. Sambri and N. Armaroli, *Inorg. Chem.*, 2014, **53**, 7709.
52. G. G. Shan, H. B. Li, H. T. Cao, D. X. Zhu, Z. M. Su and Y. Liao, *J. Organomet. Chem.*, 2012, **713**, 20.
53. W.S. Huang, J. T. Lin, C. H. Chien, Y. T. Tao, S. S. Sun and Y. S. Wen, *Chem. Mater.*, 2004, **16**, 2480.
- 25 54. B. Happ, A. Winter, M. D. Hager and U. S. Schubert, *Chem. Soc. Rev.*, 2012, **41**, 2222.
55. E. C. Constable, C. D. Ertl, C. E. Housecroft and J. A. Zampese, *Dalton Trans.*, 2014, **43**, 5343.
- 30 56. E. Orselli, G. S. Kottas, A. E. Konradsson, P. Coppo, R. Frohlich, R. Frtshlich, L. De Cola, A. van Dijken, M. Buchel and H. Borner, *Inorg. Chem.*, 2007, **46**, 11082.
57. Y. Li, L. Y. Zou, A. M. Ren, M. S. Ma and J. X. Fan, *Chem.-Eur. J.*, 2014, **20**, 4671
- 35 58. L. L. Shi, Y. Liao, G. C. Yang, Z. M. Su and S. S. Zhao, *Inorg. Chem.*, 2008, **47**, 2347.
59. G. G. Shan, H. B. Li, H. Z. Sun, H. T. Cao, D. X. Zhu and Z. M. Su, *Dalton Trans.*, 2013, **42**, 11056.
60. R. A. Marcus, *J. Chem. Phys.*, 1956, **24**, 966.
- 40 61. R. Marcus, *Rev. Mod. Phys.*, 1993, **65**, 599.



Highly efficient blue emitting cationic Ir(III) complex based on 1,2,4-triazole-pyridine ligand modified by simple methyl moiety was reported.